Integrative Medicine Research 13 (2024) 101041

Contents lists available at ScienceDirect

Integrative Medicine Research

journal homepage: www.elsevier.com/locate/imr

Original Article

Exploring the potential effect of electroacupuncture on cardiovascular function and lipid profiles in spontaneously hypertensive rats

Hye-Yoom Kim [a,1], Sarah Shin [b,1], Jung-Joo Yoon [a], You-Mee Ahn [b], Ji-Hye Song [c], Da-Som Lee [c], Ji-Yeun Park [c], Ho-Sub Lee [a,*], Jeeyoun Jung [b,**]

[a] Hanbang Cardio-renal Research Center & Professional Graduate School of Oriental Medicine, Wonkwang University, Iksan, South Korea
[b] KM Science Research Division, Korea Institute of Oriental Medicine, Daejeon, South Korea
[c] College of Korean Medicine, Daejeon University, Daejeon, South Korea

ARTICLE INFO

Keywords:
Hypertension
Lipid profiles
Spontaneously hypertensive rats
Electroacupuncture

ABSTRACT

Background: Investigating the effects of electroacupuncture (EA) treatment on cardiovascular function and aortic lipid profiles in spontaneously hypertensive rats (SHR) constitutes the foundational focus of this study. The overarching goal is to comprehensively elucidate the alterations brought about by EA treatment and to assess its potential as an alternative therapy for hypertension.

Methods: Consecutive EA treatments were administered to SHR, and the effects on systolic blood pressure, cardiac function, and hypertension-related neuronal signals were assessed. Aortic lipid profiles in vehicle-treated SHR and EA-treated SHR groups were analyzed using mass spectrometry-based lipid profiling. Additionally, the expression of Cers2 and GNPAT, enzymes involved in the synthesis of specific aortic lipids, was examined.

Results: The study demonstrated that consecutive EA treatments restored systolic blood pressure, improved cardiovascular function, and normalized hypertension-related neuronal signals in SHR. Analysis of the aortic lipid profiles revealed distinct differences between the vehicle-treated SHR group and the EA-treated SHR group. Specifically, EA treatment significantly altered the levels of aortic sphingomyelin and phospholipids, including very long-chain fatty acyl-ceramides and ether phosphatidylcholines. These changes in aortic lipid profiles correlated significantly with systolic blood pressure and cardiac function indicators. Furthermore, EA treatment significantly altered the expression of Cers2 and GNPAT.

Conclusions: The findings suggest that EA may influence cardiovascular functions and aortic lipid profiles in SHR.

1. Introduction

Hypertension poses a significant global health risk, contributing to conditions such as ischemic heart disease, stroke, chronic kidney disease, and dementia.[1,2] Efforts to effectively manage hypertension as a chronic condition are paramount. Currently, conventional treatments primarily focus on achieving optimal blood pressure levels through pharmaceutical interventions, with well-defined therapeutic mechanisms. While these medications rarely cause life-threatening side effects, they may lead to various adverse reactions such as dry cough, edema, flush, dizziness, diarrhea, headache, abdominal pain, increased urination, rapid pulse, and wheezing/shortness of breath. These adverse effects can significantly impact patients' daily lives.[3,4] As an alternative approach, the Traditional Chinese Medicine (TCM) and the Traditional Korean Medicine (TKM) offers a promising avenue for alleviating hypertension while potentially mitigating the side effects and toxicity associated with prolonged pharmaceutical use.

Acupuncture, practiced for thousands of years in TCM and TKM, stimulates specific points on the skin known as acupoints to treat various diseases.[5] Currently, acupuncture is recognized by the World Health Organization (WHO)[6] as a management strategy for many conditions, including hypertension.[7] Numerous clinical and non-clinical studies have demonstrated the effectiveness of acupuncture in reducing hypertension.[8] Electroacupuncture (EA), a modern variation of acupuncture, is gaining attention for its potential as an electroceutical. EA at the PC6 acupoint has shown promising results in improving or alleviating cardiovascular disorders such as hypertension,[7–8] myocardial infarction, and myocardial ischemia, by influencing endogenous opioids and modulating the autonomic nervous system.[8–9] However, the precise therapeutic

* Corresponding author at: Hanbang Cardio-Renal Syndrome Research Center Department of Herbal Resources, Professional Graduate School of Korean Medicine Wonkwang University, 460 Iksan-daero, Iksan 54538, South Korea.
** Corresponding author at: KM Science Research Division Korea Institute of Oriental Medicine, 1672, Yuseong-daero, Yuseong-gu, Daejeon, South Korea.
E-mail addresses: host@wku.ac.kr (H.-S. Lee), jjy0918@kiom.re.kr (J. Jung).
[1] These authors contributed equally to this work.

https://doi.org/10.1016/j.imr.2024.101041
Received 27 June 2023; Received in revised form 22 March 2024; Accepted 26 March 2024
Available online 27 March 2024

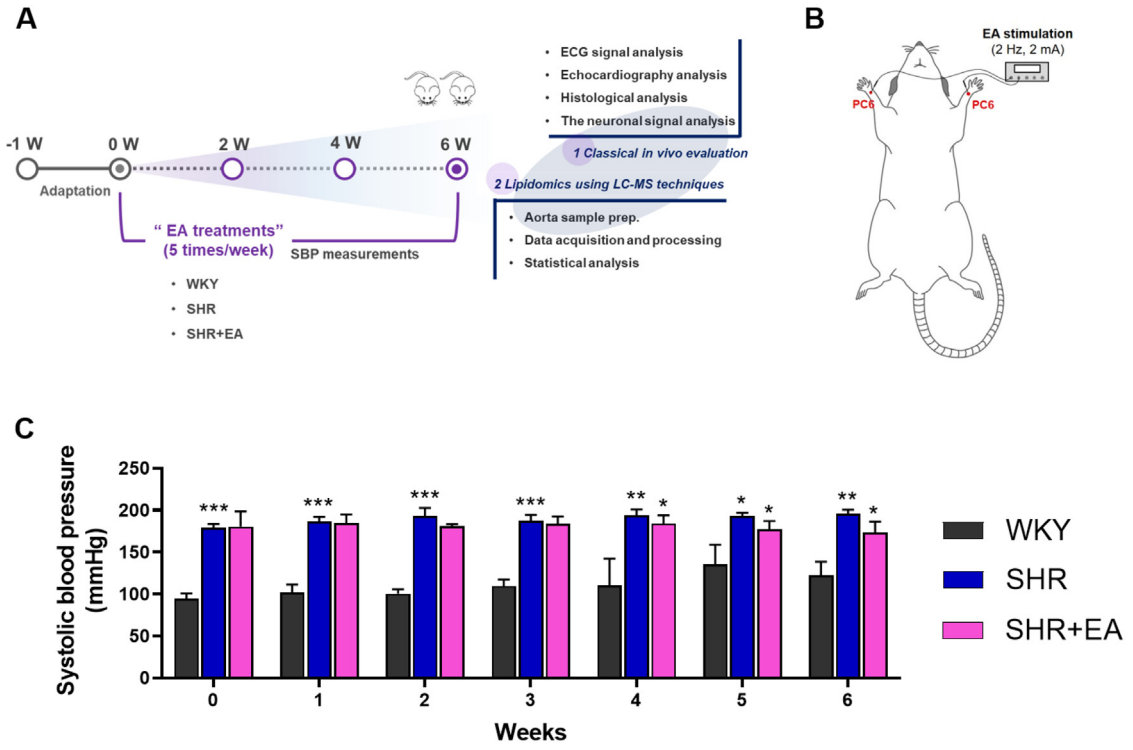

Fig. 1. Six consecutive weeks of electroacupuncture treatment decreased the systolic blood pressure in SHR. (A) Schematic of the experimental design and (B) EA stimulation points. (C) Changes in systolic blood pressure. Data were expressed as means ± *S.E.* $^{*}p < 0.05$, $^{**}p < 0.01$, $^{***}p < 0.001$. EA, electroacupuncture; WKY, Wistar-Kyoto rat; SHR, spontaneously hypertensive rat; SHR+EA, EA-treated SHR; ECG, electrocardiogram; SBP, systolic blood pressure.

mechanisms and metabolic changes associated with EA treatment of hypertension remain to be fully understood.

Hypertension presents a multifaceted cardiovascular challenge characterized by consistently elevated blood pressure levels, with implications ranging from heart disease, stroke, to kidney failure.[1–4] Understanding the intricate connections between lipid metabolism and cardiovascular health is crucial in recognizing the involvement of lipid profiles in hypertension.[10] Given the notable impact of dyslipidemia on hypertension and cardiovascular health, delving into lipid profiles among individuals with hypertension becomes crucial for identifying potential therapeutic avenues with caution.[11] In particular, the introduction of high-resolution mass spectrometry has enabled the high-throughput analysis of various lipids, allowing for the screening of changes in lipid status and identification of biomarkers in several diseases.[12] This advancement has drawn attention to the association between metabolite profiles and blood pressure in patients with hypertension.[13–14] EA, a modality of acupuncture involving electrical stimulation, has attracted attention for its purported cardiovascular benefits, including potential effects on lipid metabolism. Hence, the examination of lipid profiles in hypertensive animal models undergoing EA treatment becomes pertinent to grasp the mechanisms behind EA's therapeutic potential and its conceivable influence on lipid metabolism.

In this study, we explored the impact of EA treatment on cardiovascular function and neuronal signals associated with hypertension, focusing on spontaneously hypertensive rats (SHR). We employed ultra-high-performance liquid chromatography quadrupole time-of-flight mass spectrometry (UHPLC-QTOF-MS) to analyze the lipid profiles of the aorta, aiming to elucidate alterations induced by EA treatment. To semi-quantify potential biomarkers, stable isotope standards were utilized for each lipid class to enable matrix-matched calibration. Additionally, we assessed the mRNA expression levels related to the regulation of candidate lipid species to validate the changes induced by EA treatment in the lipid profiles of SHR.

2. Methods

2.1. EA intervention in SHR: experimental protocol

This study was performed using 8-week-old male Wistar-Kyoto rats (WKY, 180–190 g, SLC Inc., Shizuoka, Japan) and SHR (180–190 g, SLC Inc., Shizuoka, Japan). The rats were housed in individual cages in a controlled environment with 15~25 °C relative humidity, and a light/dark cycle of 12/12 h. The experimental animals were divided into three groups (n = 5 per group): vehicle-treated WKY, vehicle-treated SHR, and EA-treated SHR. The rats in all groups were anaesthetised via inhalation of 1.5 % isoflurane in 95 % oxygen and 5 % carbon dioxide. Hand acupuncture needles (length, 8 mm; diameter, 0.18 mm, Dong-Bang Medical, Seongnam, Korea) were inserted into the PC6 acupoints of anaesthetised rats. To stimulate the acupoints, the needles were connected to an electrical stimulator (SD9, Grass Instruments, Norfolk, MA, USA) with the output set to continuous waves at intensities of 2 Hz and 2 mA (Fig. 1A and B). In the EA-treated SHR group, EA was performed for 20 min five times per week for six weeks under anesthesia, whereas in the WKY and SHR groups, the same anesthesia was administered without EA treatment. Animal studies were approved by the Animal Ethics Committee of Wonkwang University (WKU20–26), and all experiments were conducted in compliance with the ARRIVE Guidelines[16] for the Care and Use of Laboratory Animals. All methods were performed in accordance with relevant guidelines and regulations. Additionally, informed consent was obtained from all authors.

2.2. Hypertension-Related cardiac functions analysis: blood pressure measurements and electrocardiograms

Noninvasive blood pressure measurements were performed using a tail-cuff CODA^{TM} High Throughput System (Kent Scientific Corporation, Torrington, CT, USA). After acclimatization on a warm pad with a heat-

ing function for 10 min, a blood pressure cuff was wrapped around the tail, and the blood pressure was measured 20 times to obtain an average value. Systolic blood pressure (SBP) measurements were performed once a week for all groups. Electrocardiogram (ECG) signals were measured for approximately 5 min by inserting three electrodes under the skin of both arms and legs of anaesthetised rats and connecting them to an ECG amplifier at 2 MHz. Data for the measured signals were recorded using a PowerLab system (ADInstruments, Bella Vista, NSW, Australia).

2.3. Echocardiography analysis

Cardiac function was analysed by recording the M-mode using a high-resolution ultrasound imaging system (VINNO 6; Vinno Corporation, Suzhou, China). Echocardiography was used to measure and record the left ventricular posterior wall thickness at ejection fraction (EF), fragment shortening (FS), and left ventricular posterior wall thickness at end systole (LVPWs).

2.4. Measurement of isometric force in the aorta

All groups of rat aortic rings were placed in an organ bath filled with 5 mL of Krebs solution with oxygenated 95 % O2 and 5 % CO2. After the prepared aortic ring was equilibrated for 60 min, contraction was induced with phenylephrine (1 μM) and the relaxation effect was confirmed by treatment with acetylcholine (ACh). Isometric tension changes were recorded using a transducer connected to a Grass Polygraph (Grass FT 03, Grass Instrument Co., Quincy, MA, USA).

2.5. Histological analysis of the thoracic aorta and left ventricle tissues

The thoracic aorta and left ventricle tissues were fixed in 10 % neutral buffered formalin (10 % NBF, HT501128, Merck, Darmstadt, Hessen, Germany) solution for 24 h. Fixed tissues were embedded in paraffin, separated into thin 3–6 μm sections, and attached to slides. The slides were stained with haematoxylin and eosin (H&E) and Masson's trichrome stain kit (Masson Trichrome stain, BBC Biochemical, Mt Vernon, WA, USA) for histopathological comparisons and analysed using light microscopy (EVOSTM M5000, Thermo Fisher Scientific, Bothell, WA, USA).

2.6. Hypertension-Related neuronal signal analysis

Rat brains were extracted, post-fixed in 4 % paraformaldehyde (PFA, Sigma Aldrich, St. Louis, MO, USA) at 4 °C, and then stored overnight in a gradient of 10–30 % sucrose solution. The brains were then cut into coronal sections of 40 μm thickness using a cryostat (CM3050S, Leica Microsystems, Nussloch, Germany) and stored at 4 °C in an antifreeze storing solution. For immunohistochemistry, brain tissues were pretreated with the following primary antibodies: c-Fos (1:250; Abcam, Cambridge, MA, USA) and angiotensin-converting enzyme (ACE) (1:100, Santa Cruz Biotechnology, Dallas, TX, USA). Stained brain sections were mounted and observed under a microscope (Nikon, Minato, Japan). The number of stained cells in each brain region was counted within a square of 300 μm × 300 μm, and the mean values of the left and right regions were calculated. For immunofluorescence, brain tissues were pretreated with primary antibodies against angiotensin I receptor (AT1, 1:50, Enzo Life sciences, Farmingdale, NY, USA) and angiotensin II receptor (AT2, 1:50, Enzo Life sciences, Farmingdale, NY, USA). Brain tissues were observed under a fluorescence microscope (Nikon, Minato, Japan). Detailed immunostaining procedures are shown in the Supplementary Information (**Method S1**)

2.7. Lipid profiling: aorta analysis: lipid profiles analysis and lipid quantification

For lipid profiling, 10 mg of aortic vessel was extracted and evaporated, and the resulting lipid pellet was reconstituted with 200 μL of an isopropanol-acetonitrile mixture (4:1, v/v). The detailed sample preparation procedures are presented in the Supplementary material (Method S2).

The lipid composition of the biological samples was simultaneously analysed using UHPLC (1290 Infinity II LC system, Agilent Technologies, Santa Clara, CA, USA) connected to a Q-TOF-MS (6546 Q-TOF system, Agilent Technologies) system. The mobile phase consisted of 10 mM ammonium acetate (or ammonium formate) in an acetonitrile-water mixture (4:6, v/v; solvent A) and 10 mM ammonium acetate (or ammonium formate) in acetonitrile-isoproparol (1:9, v/v; solvent B) in positive (or negative) ion mode. The detailed experimental conditions and parameters are summarised in Table S1. In addition, we conducted four consecutive iterative ms/ms acquisitions and all ion fragmentation acquisitions by pooling quality samples to expand the coverage of lipid profiles. The acquired UHPLC-QTOF-MS data for non-targeted lipid composition analysis were processed using MS-Dial (Ver 4.70, http://prime.psc.riken.jp/) to detect features, perform alignments, and generate peak tables of *m/z* and retention times in the samples. The system stability and reproducibility of the analytical method in the main batch were assessed with a quality control (QC) sample, comprising a pool of all samples, and a method blank sample was injected repeatedly between every ten runs. The resulting plots were densely clustered in the principal component analysis scatter plots (data not shown). Features with more than 20 % coefficient variation were removed from statistical analysis.

The surrogate biomarkers were semi-quantified using a previously described method.[17] Lipid quantification was performed using calibration curves of pooled QC samples spiked with known concentrations of stable isotope lipid standards (SPLASH® LIPIDOMIX® Mass Spec Standard). phosphatidylcholine (PC) 15:0_18:1(d7), phosphatidylethanolamines (PE) 15:0_18:1 (d7), sphingomyelin (SM) 18:1, and 2O/18:1 (d9) were used to analyze the relative concentrations of PC, PE, and SM, respectively (Fig. S1).

2.8. Multivariate analysis

Multivariate statistical analyses were performed using the unit variance scale in SIMCA-P^+ (version 16.0; Umetrics, Umea, Sweden). The partial least squares discriminant analysis (PLS-DA) model was used as a discriminant method to maximize the covariance between the measured data and response variables in the three groups. The reliability of the PLS-DA model was validated by a 100-repeated permutation test and a CV-ANOVA test using SIMCA-P software (version 17.0). Lipid metabolites with variable importance in the projection (VIP) score > 1.0 were considered as the metabolites responsible for the differences between the WKY, SHR, and SHR+EA groups. Pavlidis template matching (PTM) analyses were conducted based on the Pearson correlation between the template and selected lipid metabolites using Multi Experiment Viewer (version 4.9.0. MeV, TIGR, Washington, DC, USA), and data visualization was conducted using GraphPad Prism (version 9.0; GraphPad Software, La Jolla, CA, USA).

2.9. Real-Time quantitative RT-PCR

A Qiagen RNeasy^{TM} Plus mini kit was used for RNA isolation, and the quality of the results was assessed by measuring the 260/280 nm ratio using a UV-spectrophotometer. Real-time quantitative RT-PCR analysis was carried out in a 96-well plate using the Opticon MJ Research instrument (Bio-Rad Inc.) and the optimised standard SYBR Green 2-step qRT-PCR kit protocol (DyNAmo^{TM}, Finnzymes, Finland). The specific sense and antisense primers for ceramide synthase 2 (Cers2) and glyceronephosphate O-acyltransferase (GNPAT) are listed in Table S2. PCR was initiated at 95 ˚C for 15 min (hot start) to activate AmpliTaq polymerase, followed by a 45-cycle amplification (denaturation at 94 ˚C for 20 s, annealing at 60 ˚C for 30 s, extension at 72 ˚C for 60 s, and plate reading at 60 ˚C for 10 s). The temperature of the PCR products was

increased from 65 °C to 95 °C at a rate of 0.2 °C/1 s, and the resulting data were analysed using the software provided by the manufacturer.

3. Results

3.1. Six consecutive weeks of EA-Treatment decreased the systolic blood pressure and restored hypertension-related cardiac functions in SHR

The overall schematic of the experimental design (A) and diagrams of EA stimulation at the PC6 acupoints (B) are shown in Fig. 1. At treatment initiation, SBP in the SHR and SHR+EA groups was significantly higher than that in the WKY group. Of total 6 weeks of EA treatment period, from after 4 consecutive weeks of EA treatment, SBP showed a decreasing trend in the SHR+EA group which was significantly lower than that of the SHR group after 6 weeks of EA treatment (WKY, 107.4 ± 2.8; SHR, 196.0 ± 2.0; SHR+EA, 171.4 ± 5.0 mmHg, $p < 0.01$) (Fig. 1**C**). ECGs were performed to investigate the electrocardiographic parameters of SHR treated with EA. As shown in Fig. 2A and B, ECG parameters such as heart rate, RR interval, and QRS interval were suppressed in the SHR group compared to those in the WKY group. Conversely, after six consecutive EA treatments, the suppressed ECG parameters improved in the SHR group. However, these trends did not reach the statistical thresholds. As shown in Fig. 2C, measurements of left ventricular systolic function, which were evaluated using M-mode representative echocardiography images, showed that the decreased left ventricular fragment EF and FS values in the SHR were improved by six consecutive weeks of EA treatment (Fig. 2 Da and 2Db). Moreover, the elevated LVPWs levels in the SHR group were significantly decreased in the SHR+EA group ($p < 0.05$) after six weeks of consecutive treatment (Fig. 2Dc). H&E staining (Fig. 2Ea) was used to examine the cardiovascular morphological changes, and the results indicated that the blood vessels were thicker in the SHR group than in the WKY group; however, after six consecutive weeks of EA treatment, the blood vessels were thinner in the SHR+EA group than in the SHR group. In the vascular relaxation experiment, ACh-induced concentration-response relaxation in the aorta was significantly suppressed in the SHR group (35.2 ± 2.4 %, $p < 0.001$) compared to the WKY group (91.7 ± 1.0 %) and significantly recovered in the SHR+EA group (52.7 ± 2.5 %, $p < 0.001$) after six consecutive weeks of EA treatment (Fig. 2 Eb). Moreover, the E_{max} (WKY, 35.2 ± 2.4; SHR, 91.7 ± 1.0; SHR+EA, 52.7 ± 2.5, $p < 0.001$) and -log EC_{50} (WKY, 8.41 ± 0.10; SHR, 7.76 ± 0.08; SHR+EA, 8.18 ± 0.07, $p < 0.01$) values recovered significantly after six consecutive weeks of EA treatment (Fig. 2Ec).

3.2. Six consecutive weeks of EA-Treatment changes the hypertension related-neuronal signal in SHR

We determined the changes in c-Fos expression in key brain regions associated with hypertension after six consecutive weeks of EA treatment in the SHR model. As shown in Fig. 3, c-Fos expression was significantly increased in the nucleus accumbens NAc ($p < 0.05$), paraventricular nucleus (PVN $p < 0.01$), and rostral ventrolateral medulla RVLM ($p < 0.05$) brain regions of the SHR group compared with the WKY group; however, c-Fos expression was significantly decreased after EA treatment ($p < 0.01$ in the NAc and PVN and $p < 0.05$ in the RVLM vs. SHR) (Fig. 3A). We observed changes in ACE expression and found that it was significantly increased in the NAc ($p < 0.01$), PVN ($p < 0.001$), and RVLM ($p < 0.01$) brain regions of the SHR group compared to the WKY group; however, they were all significantly decreased after six weeks of EA treatment ($p < 0.01$ in the NAc, $p < 0.001$ in PVN and $p < 0.05$ in the RVLM vs. SHR) (Fig. 3B). In the brain, AT1 and AT2 show contrasting expressions in the regulation of blood pressure. In the PVN brain region of the SHR group, AT1 expression was increased compared to that in the WKY group, but AT2 expression was decreased. These changes were altered after six weeks of EA treatment (Fig. 4A and B).

3.3. Consecutive EA-Treatment induces aortic lipid pattern alterations in the SHR

From the above results, we observed that EA treatment at the PC6 acupoint changed hypertension-related cardiac functions and neuronal signals. We then analysed the lipid extracts obtained from the aortic vessels of all groups using a UHPLC-QTOF MS system coupled with multivariate analyses to identify the aortic lipid composition changes induced by EA treatment in the SHR model (Fig. 5). Representative total ion chromatograms (TICs) of aortic lipid extracts after EA treatment for six consecutive weeks are shown in Fig. 5C and 5D (left panels, positive and negative, respectively). Fourth sequential iterative exclusion acquisitions, which can be used to identify the features of a given sample, were applied to the pooled samples, which increased the coverage of tentatively identified lipids from 219 to 500 in positive mode and from 74 to 78 in negative mode (Fig. 5B). The PLS-DA score plot of the experimental groups revealed that each cluster (WKY, SHR, and SHR + EA) was clearly separated. In particular, the SHR group was clearly separated from the WKY group by the first component, whereas the SHR + EA group was slightly shifted from the WKY cluster to the SHR cluster in both positive ($R^{2X} = 0.504$, $R^{2Y} = 0.692$, $Q^2 = 0.467$) and negative ($R^{2X} = 0.705$, $R^2Y = 0.683$, $Q^2 = 0.467$) modes (Fig. 5C and D, middle). Further, the performance of the PLS-DA model was validated by 100-fold repeated permutation tests (Fig. 5C and D, right) and CV-ANOVA results ($p = 0.015$ for positive mode and $p = 0.010$ for negative mode).

3.4. Identification of key altered lipids following six weeks of EA-Treatment in SHR

Significantly altered lipid metabolites were selected via double validation. First, 62 important lipid features (48 in positive and 14 in negative modes) that showed significant differences among the three groups were chosen according to the following criteria: (a) VIP > 1.0 based on PLS-DA and (b) statistical differences of $p < 0.05$, one-way ANOVA followed by Tukey's HSD *post-hoc* test. Then, PTM analysis was applied to determine the lipid metabolites that had similar expression patterns to the specified templates (WKY:0, SHR:1, SHR + EA:0) among the three groups. The threshold criterion for matching was a correlation coefficient $|R| > 0.75$. The results tentatively identified a total of 48 lipid features (37 in the positive mode and 11 in the negative mode) as ceramides (Cer), diacylglycerol (DG), sphingomyelin (SM), phosphatidylethanolamine (PE), phosphatidylcholine (PC), and triacylglycerol (TG), which were matched with the designated template (Fig. 6Aa and 6Ab)

3.5. Identification of selected lipid features after six consecutive weeks of EA-Treatment in SHR

To identify the selected lipid features, we verified the separation, retention time, and MS/MS pattern of candidates and ultimately confirmed 32 (24 for positive and 8 for negative modes: (i) positive: Cer 42:1, 2O|Cer 18:1, 2O/24:0; (ii) negative: SM 42:3;2O|SM 24:0;2O/18:3; (iii) both modes: PC 32:1|PC 16:0_16:1) (Fig. 6B and Table 1). We observed that several plasmanyl PC (PC–O) levels were increased in the SHR group and were decreased by EA treatment. Different ether-linked PEs (PE-P and PE-O) were also detected. To determine plasmenyl and plasmanyl ether-linked phospholipids, we confirmed the MS/MS fragmentation pattern. As shown in Fig. 6C, in the PC–O mass spectra, the precursor ion of PC O- was detected at *m/z* 746, and it decomposed to product ions at *m/z* 563, 378, and 184, which corresponded to the loss of a phosphocholine head group from the precursor ion, *sn*2 acyl chain $[RC=O]^+$, and phosphocholine head group, respectively. The precursor ion of PE O- observed at *m/z* 774 was primarily fragmented into *m/z* 464 (loss of *sn*2 acyl chain as ketene from the precursor ion), *m/z* 446 (neutral loss of *sn*2 RCOOH group from the precursor ion), *m/z* 327 (*sn*2 RCOO- ion), and *m/z* 283 (loss

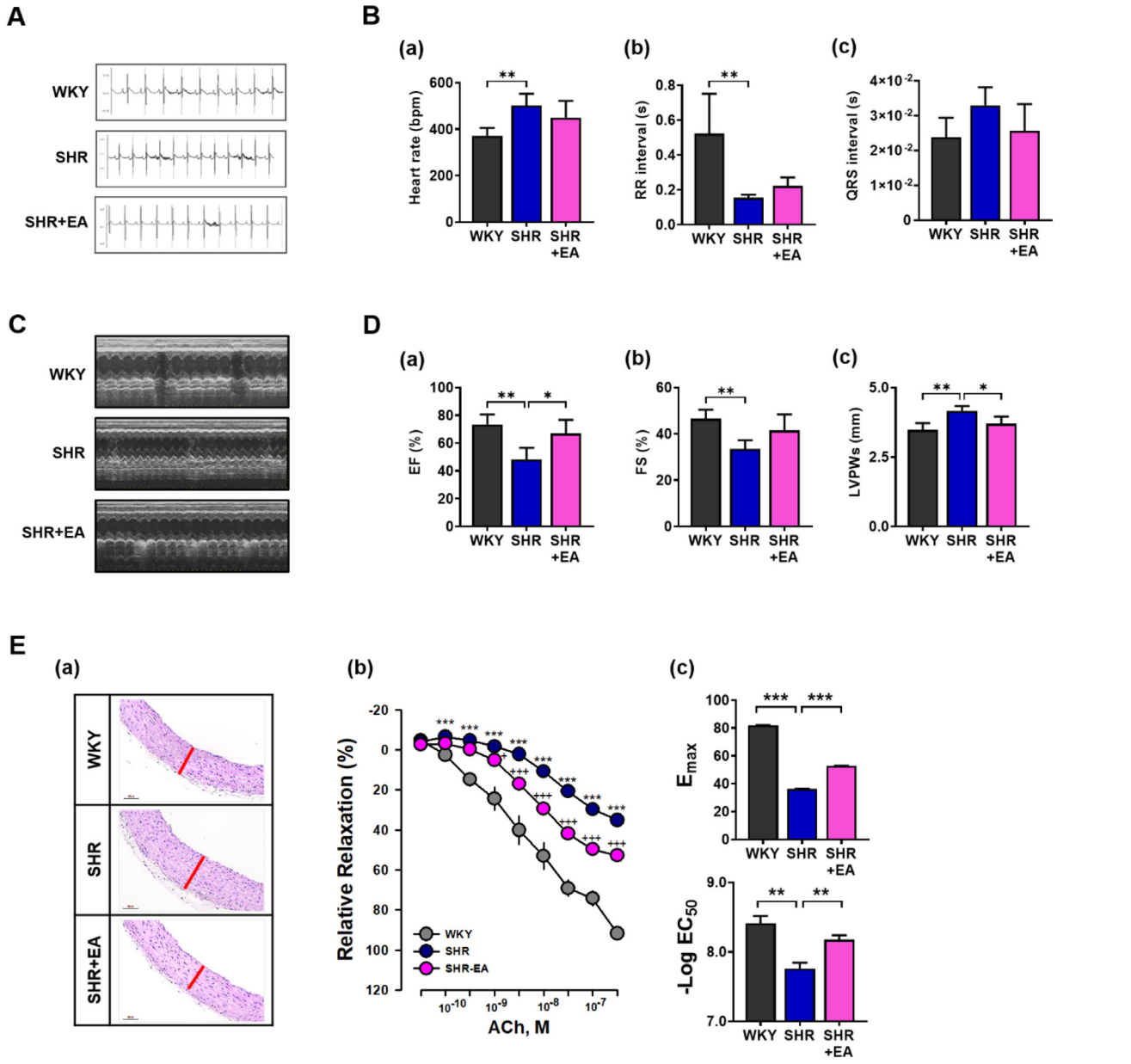

Fig. 2. Six consecutive weeks of electroacupuncture treatment ameliorated hypertension related cardiovascular functions. (A) Electrocardiograms of the WKY, SHR, and SHR+EA groups. Electrocardiogram parameters, such as (Ba) heart rate, (Bb) RR interval, and (Bc) QRS interval analysis values, were recorded. (C) Echocardiographic images (M mode) of the WKY, SHR, and SHR+EA groups. Analysis values of the (Da) ejection fraction, (Db) fractional shortening, and (Dc) left ventricular posterior wall thickness at end systole. (Ea) Representative images of H&E-stained thoracic aorta to confirm the histopathological changes. The red line in the thoracic aortic staining image represents the comparison of vessel thickness. (Eb) Cumulative concentration-response relaxation curves for acetylcholine induction of each group in the aorta. (Ec) Emax and EC50 values for acetylcholine-induced relaxation. Data are expressed as the means ± *S*.E. $^{*}p < 0.05$, $^{**}p < 0.01$, $^{***}p < 0.001$. EA, electroacupuncture; WKY, Wistar-Kyoto rat; SHR, spontaneously hypertensive rat; SHR+EA, EA-treated SHR; RR interval, QRS to QRS or inter-beat intervals; QRS interval, a combination of the Q wave, R wave and S wave; "QRS complex", ventricular depolarization; EF, ejection fraction; FS, fractional shorting; LVPWs, left ventricular posterior wall thickness at end systole; ACh, acetylcholine; H&E, hematoxylin and eosin.

of CO_2 from *sn*2 RCOO- ion) (Fig. 6C). Distinguishingly, in the PE P-mass spectra (Fig. 3**C**), the precursor ion of PE P- revealed at *m/z* 776 was mainly fragmented into *m/z* 635, 526, 392, 385, and 294, corresponding to the neutral loss of phosphoethanolamine, loss of a plasmenyl group (RC=CH2) from the precursor ion, neutral loss of the glycerol backbone with an *sn*2 acyl group from the precursor ion, loss of two neutral products, including a plasmenyl group as an alcohol and a phosphorous atom with a ring compound, from the precursor ion at the *sn*2 site, and neutral loss of H_3PO_4 from the sn1 plasmenyl group.

3.6. Changes in selected lipid metabolites during six consecutive weeks of EA-Treatment in SHR

To measure the levels of the selected lipid candidates, semi-quantification was performed using class-specific calibration curves with deuterated standards. The levels of PCs (PC 30:0, 32:1, 32:2, 34:0, 36:1, 38:2, 38:4, 38:5, 40:4, and 40:6), PC O- (PC O-32:1, 34:0, 34:1, 38:4, and 38:5), and PEs (PE O-40:7, PE P 40–5, P-40:6) were significantly higher in the SHR group than in the WKY group, whereas they were significantly decreased in the SHR + EA group compared to those

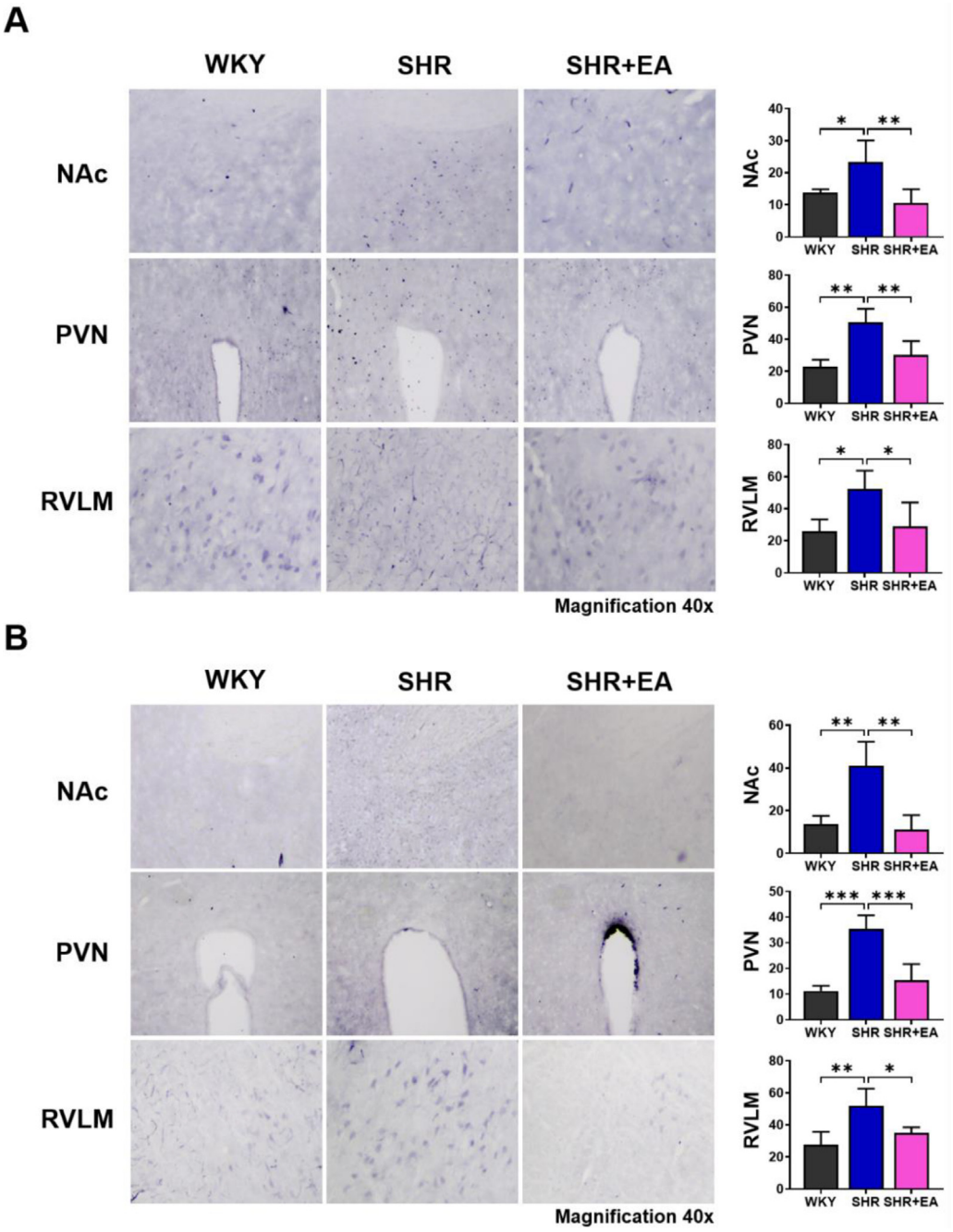

Fig. 3. Changes in c-Fos and angiotensin-converting enzyme expression following electroacupuncture treatment in NAc, PVN, and RVLM of brain. (A) Number of c-Fos-positive cells in the NAc, PVN, and RVLM regions. (B) Number of ACE-positive cells in the NAc, PVN, and RVLM regions. Data are expressed as the means ± S.E. $^{*}p < 0.05$, $^{**}p < 0.01$, $^{***}p < 0.001$. EA, electroacupuncture; WKY, Wistar-Kyoto rat; SHR, spontaneously hypertensive rat; SHR+EA, EA-treated SHR; ACE, angiotensin-converting enzyme; NAc, nucleus accumbens; PVN, paraventricular nucleus; RVLM, rostral ventrolateral medulla.

in the SHR group (Fig. 7A and Fig. S2). Similarly, levels of SMs (SM 34:1, 34:2, 36:1, 42:1, 42:2, and 42:3) and Cer 42:1 were higher in the SHR group than in the WKY group. Of these, only a few SMs (SM 42:1, 42:2, and 42:3) and Cer 42:1 were significantly decreased by consecutive EA treatment (Fig. 7B and Fig. S2).

3.7. Lipid profiles analysis of the aorta reflects the effect of repetitive EA-Treatment in SHR

We conducted a Spearman correlation analysis between lipid metabolites and cardiac function indicators, such as SBP, EF, FS, and LVPWs, to identify the lipid profiles parameters that indicate the effect of EA treatment on SHR. As shown in Fig. 8A, most of the selected lipid metabolites were positively correlated with SBP and LVPWs, whereas they were negatively correlated with EF and FS. Several ether-linked phospholipids, SMs, and Cer, with very long fatty acid chains, have been observed. Thus, we investigated the mRNA expression of GNPAT, which participates in the initial steps of ether PC synthesis.[18] The mRNA expression of GNPAT in the SHRs was higher than that in the WKY group, whereas the expression was lower in the SHR + EA group than in the SHR group, indicating that EA treatment modulated ether PC synthesis (Fig. 8B). Moreover, the mRNA expression of Cers2, which produces ceramides with very long C24- and C22-fatty acyl (VLCFA), was significantly altered by EA treatment (Fig. 8C).[19]

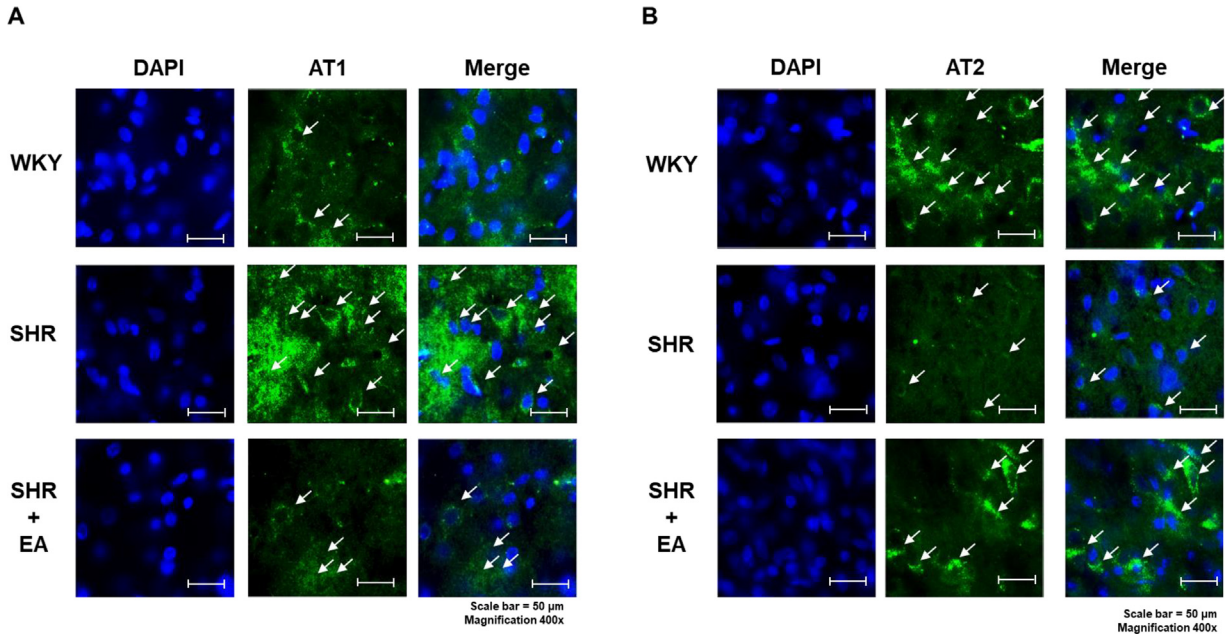

Fig. 4. Changes in hypertension-related factors following electroacupuncture treatment in different brain regions. (A) AT1 and (B) AT2 expression in the paraventricular nucleus brain region observed using immunofluorescence (scale bar = 50 μm). EA, electroacupuncture; WKY, Wistar-Kyoto rat; SHR, spontaneously hypertensive rat; SHR+EA, EA-treated SHR; PVN, paraventricular nucleus; AT1, Angiotensin II receptor subtype 1; AT2, Angiotensin II receptor subtype 2; DAPI, 4′,6-diamidino-2-phenylindole.

Table 1
List of 21 significantly altered metabolites in both polarity modes.

Modes	Lipids	Formula	Adducts	Molecular weight	Theoretical *M/Z*	Observed *M/Z*	△ PPM	RT	Fragment ions*
Positive	Cer 42:1;2O |Cer 18:1;2O/24:0	C42H83NO3	[*M* + *H*–H_2O]+	649.6373	632.634	632.6351	1.83	16.12	360.2163, 264.2697
	PC 32:1 |PC 16:0_16:1	C40H78NO8P	[*M* + *H*]+	731.5465	732.5538	732.5563	3.51	11.45	496.3367, 476.3098, 184.0736
	PC 32:2 |PC 16:1_16:1	C40H76NO8P	[*M* + *H*]+	729.5309	730.5081	730.5388	0.96	10	494.3127, 476.3135, 184.0734
	PC 34:0 |PC 16:0_18:0	C42H84NO8P	[*M* + *H*]+	761.5934	762.6007	762.6029	2.88	14.82	524.3631, 478.3287, 184.0734
	PC 36:1 |PC 18:0_18:1	C44H86NO8P	[*M*+Na]+	787.6091	810.5983	810.5999	1.88	14.87	627.5384, 184.0728, 146.9832
	PC 38:2	C46H88NO8P	[*M* + *H*]+	813.6247	814.632	814.6325	0.6	14.97	184.0732
	PC 38:4	C46H84NO8P	[*M*+Na]+	809.5934	832.5827	832.5834	0.89	13.31	649.5166, 149.9810, 85.0963
	PC 38:5	C46H82NO8P	[*M*+Na]+	807.5778	830.567	830.568	1.17	11.87	647.5010, 146.9891
	PC 40:4 |PC 18:0_22:4	C48H88NO8P	[*M* + *H*]+	837.6248	838.632	838.6338	2.15	14.75	506.3605, 184.0736
	PC 40:6 |PC 18:0_22:6	C48H84NO8P	[*M* + *H*]+	833.5934	834.6007	834.6008	0.14	12.21	569.3429, 506.3605, 184.0734
	PC O-32:1	C40H80NO7P	[*M* + *H*]+	717.5672	718.5745	718.5753	1.11	14.33	535.5085, 184.0733
	PC O-34:0	C42H86NO7P	[*M* + *H*]+	747.6142	748.6215	748.6224	1.15	15.23	565.5554, 184.0773
	PC O-34:1	C42H84NO7P	[*M* + *H*]+	745.5985	746.60577	746.60699	1.63	14.54	563.5398, 184.0738
	PC O-38:4	C46H86NO7P	[*M* + *H*]+	795.6142	796.6215	796.6219	0.46	14.39	613.5367, 184.0734
	PC O-38:5	C46H84NO7P	[*M* + *H*]+	793.5985	794.6058	794.6065	0.86	13.18	611.5398, 184.0734
	PE P-40:5 |PE P-18:0_22:5	C45H80NO7P	[*M* + *H*]+	777.5672	778.5745	778.5753	1.03	14.84	637.5552, 387.2884, 294.3155
	PE P-40:6 |PE P-18:0_22:6	C45H78NO7P	[*M* + *H*]+	775.5516	776.5589	776.559	0.15	14.58	635.5398, 385.2740, 294.3157
	SM 42:1;2O |SM 18:1;2O/24:0	C47H95N2O6P	[*M* + *H*]+	814.6927	815.7001	815.7022	2.62	15.82	184.0735
	SM 42:2;2O |SM 18:1;2O/24:1	C47H93N2O6P	[*M* + *H*]+	812.6771	813.6844	813.6867	2.85	15.44	184.0735
Negative	PC 30:0| PC 14:0_16:0	C38H76NO8P	[M+CH_3COO]-	705.5308	764.5447	764.5433	1.77	11.25	690.5117, 434.2677, 253.3408, 227.2012
	PE O-40:7| PE O-18:1_22:6	C45H78NO7P	[M-H]-	775.5516	774.5443	774.5436	0.94	14.59	464.3146, 327.2333

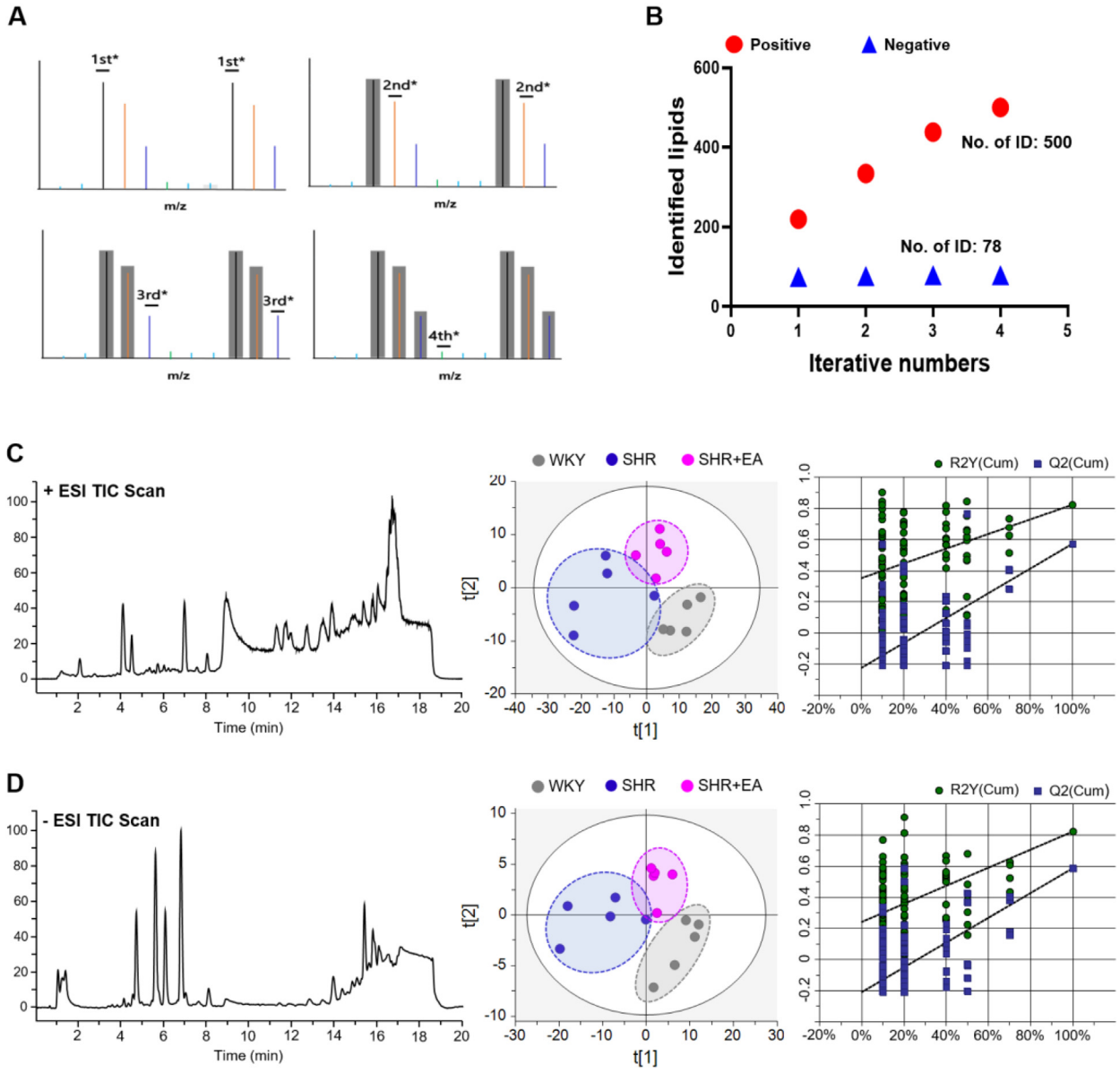

Fig. 5. Electroacupuncture treatment for six consecutive weeks alters the aortic lipid pattern in SHR. (A) Scheme of iterative MS/MS. (B) Number of identified lipid features acquired from the iterative MS/MS analysis. Representative total ion chromatograms (left), PLS-DA score plots (middle), and 100-fold permutation plots (right) derived from positive (C) or negative (D) modes of the UHPLC Q-TOF system. EA, electroacupuncture; WKY, Wistar-Kyoto rat; SHR, spontaneously hypertensive rat; SHR+EA, EA-treated SHR; MS/MS, tandem mass spectrometry; ESI TIC, electrospray ionization total-ion current; PLS-DA, partial-least-squares discriminant analysis; UHPLC Q-TOF, ultra-high performance liquid chromatography-quadrupole time-of-flight mass spectrometry.

4. Discussion

This study assessed the impact of EA treatment on cardiovascular function and neural signaling related to hypertension in SHR using classical in vivo methods and aortic lipid profiling via LC-MS. The findings suggest that EA treatment may have a potential positive effect on cardiovascular functions, such as lowering SBP, enhancing left ventricular systolic function, and potentially reducing cardiac hypertrophy. Additionally, there is a chance that EA treatment might impact the aortic lipid profile in SHR. This research aims to contribute to the understanding of acupuncture as a possible alternative treatment for hypertension, exploring its effects through various mechanisms.[20,21]

One therapeutic mechanism explored is the potential impact of EA treatment on endothelial dysfunction in cardiovascular diseases,[22] including hypertension, by potentially enhancing endothelial-derived NO biocompatibility.[23] Chronic hypertension can strain the left ventricle, leading to left ventricular hypertrophy and affecting parameters such as FS and EF on echocardiography.[24,25] Our findings suggest that six consecutive weeks of EA treatment may restore FS and EF functions, hinting at a potential improvement in left ventricular hypertrophy over the long term. Another investigated mechanism involves the renin-angiotensin-aldosterone system (RAAS), which plays a role in regulating blood pressure homeostasis, vascular responses, and is implicated in inflammation, fibrosis, and target organ damage.[26] Acupuncture has been suggested to potentially modulate levels of ACE and angiotensin II receptors (AT1R and AT2R), resulting in decreased plasma content of angiotensin II and exhibiting antihypertensive effects in various animal models.[27–29] Similarly, our study indicates that EA treatment may influence hypertension-related neuronal signals, including the expression of c-Fos, ACE, AT1R, and AT2R in key brain regions.

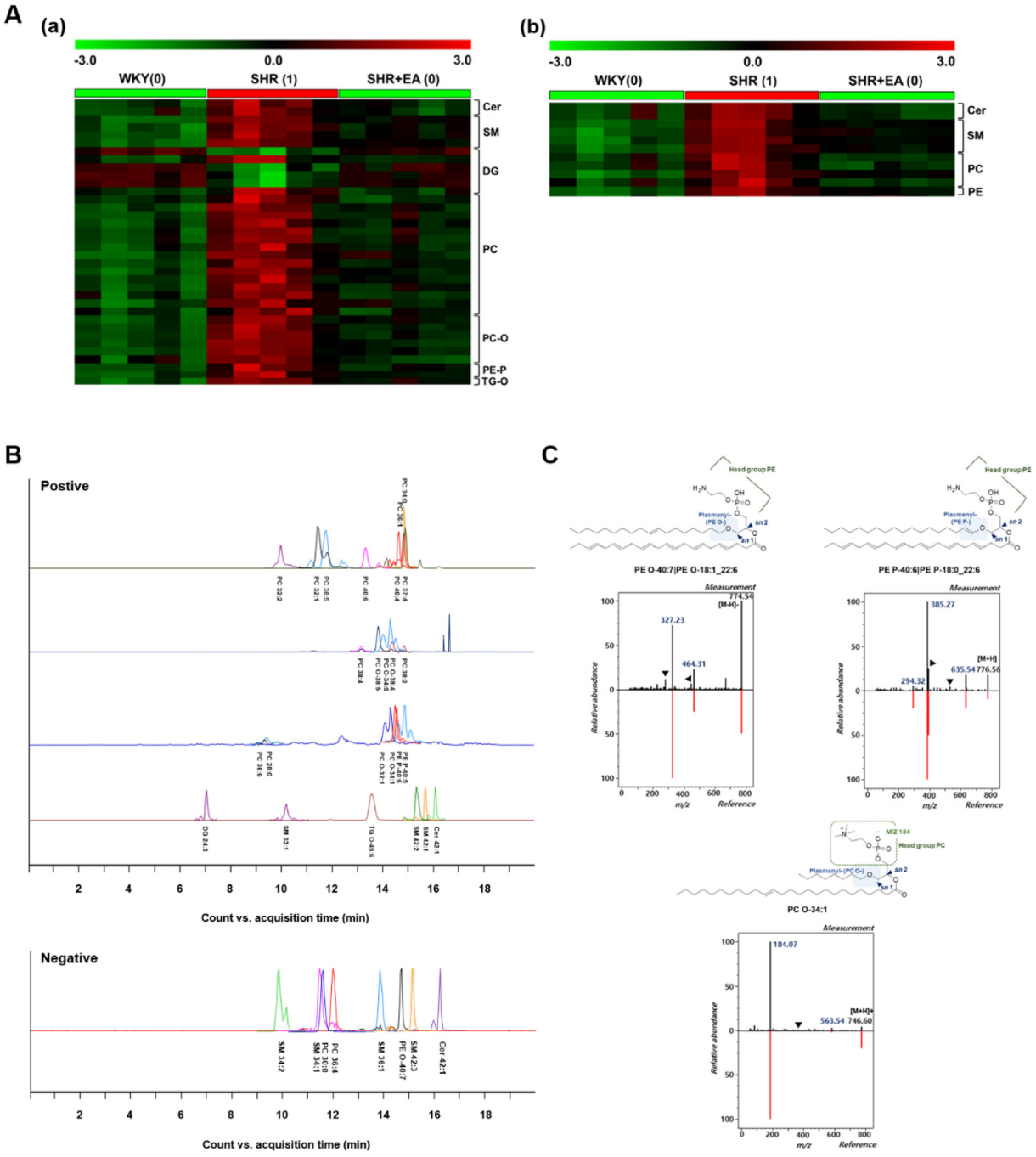

Fig. 6. Identification of significantly altered lipid metabolites in the aorta obtained from SHR treated with electroacupuncture for six consecutive weeks. PTM plots using metabolites selected from (Aa) positive and (Ab) negative modes. Threshold criterion for PTM matching: (|R|> 0.75). (B) Retention time and separation status of selected metabolites. (D) Composition of ether-linked phospholipids identified by mass fragmentation. EA, electroacupuncture; WKY, Wistar-Kyoto rat; SHR, spontaneously hypertensive rat; SHR+EA, EA-treated SHR; Cer, ceramides; DG, diacylglycerol; PC, phosphatidylcholine; PC–O, plasmanyl-phosphatidylcholine; PE, phosphatidylethanolamine; PE-O, plasmanyl-phosphoethanolamines; PE-P, plasmenyl-phosphoethanolamines; PTM, pavlidis template matching; SM, sphingomyelin; TG-O, plasmanyl-triacylglycerol.

In existing research, the focus of EA treatment on hypertension has primarily revolved around molecular biology and neurology, with a noticeable gap in studies concerning lipid profiles. Limited investigations have applied lipid profiling analyses to understand the effects of EA treatment. While Liu et al.[30] employed a metabolomics approach based on 1H NMR to uncover the therapeutic mechanism of EA and moxibustion on chronic atrophic gastritis,[29] our team previously investigated alterations in lipid metabolic patterns through lipid profiling analysis based on UHPLC-QTOF-MS in response to acupuncture. Accordingly, in this study, we investigated the changes in lipid patterns induced by EA treatment in the aorta of SHR. Particularly, sphingolipids, such as ceramides (Cers) and sphingomyelins (SMs), and phospholipids, including phosphatidylcholines (PCs) and phosphatidylethanolamines (PEs), showed significant correlations with hypertension indicators. Sphingomyelins are known to influence vascular growth through the activation of the sphingosine-1-phosphate (S1P) receptor, which is associated with the regulation of vascular tone, including the modulation of nitric oxide and the endothelium-derived hyperpolarizing factor (EDHF)-

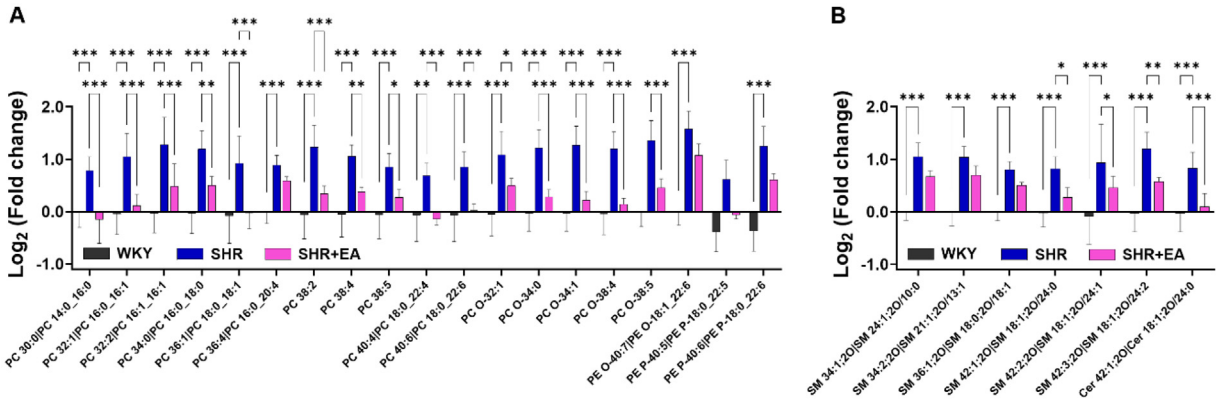

Fig. 7. Significantly altered lipid metabolites following electroacupuncture treatment on the SHR model. Statistical comparison of selected (A) phospholipids and (B) sphingolipids using semi-quantified data. $^{*}p < 0.05$, $^{**}p < 0.01$, $^{***}p < 0.001$. EA, electroacupuncture; WKY, Wistar-Kyoto rat; SHR, spontaneously hypertensive rat; SHR+EA, EA-treated SHR; Cer, ceramides; PC, phosphatidylcholine; PC–O, plasmanyl-phosphatidylcholine; PE, phosphatidylethanolamine; PE-O, plasmanyl-phosphoethanolamines; PE-P, plasmenyl-phosphoethanolamines; SM, sphingomyelin.

mediated relaxing response in the vascular system.[31,32] This aligns with previous research by Borodzicz et al.,[33] suggesting the potential significance of SM in the progression of hypertension and the possible benefits of inhibiting de novo ceramide synthesis for improving myocardial systolic function.

In this study, changes were observed in Cer d18:1/24:1 and the mRNA expression of Cers2 due to EA treatment in SHR.[19] Additionally, Spijkers et al.[34] reported elevated basal Cer levels in both SHR and humans with hypertension. Our findings aligned with this, demonstrating increased levels of Cers and SMs, particularly those with relatively low degrees of unsaturated fatty acids (< 4), in the SHR group and a subsequent decrease in the SHR + EA group. Moreover, the study highlighted the impact of saturated fatty acids on de novo ceramide synthesis, corresponding with the observed FA results, which showed an increase in aortas from the SHR group compared to those from the WKY group and a decrease in the SHR + EA group.[35] The study also revealed alterations in phospholipids, specifically PCs and PEs, showing an increase in SHR and a subsequent decrease after six weeks of consecutive EA treatment. Phospholipids, known as primary components of cell membranes, play a central role in maintaining membrane structural integrity and function.[36] Notably, several Plasmanyl PCs, containing a saturated ether moiety at the *sn*1 PC–O, were found to be altered in SHR and restored by EA treatment.[37] Plasmanyl PC, functioning as a platelet activator and an essential membrane constituent of neutrophils,[38] has been implicated in neuro-inflammatory responses,[39] which can be modulated by acupuncture treatment.[17] The study further demonstrated that EA treatment significantly altered the mRNA expression level of Cers2, responsible for producing ceramides with VLCFA and GNPAT, playing a role in the initial step of ether PC synthesis in SHR.

Emerging technologies, such as high-resolution tandem mass spectrometry coupled with UHPLC, have significantly broadened the scope of lipid profiling studies. However, despite these advancements, structural identification through MS/MS encounters limitations, as obtaining fragmentation data for all precursor ions proves challenging. Koelmel et al.[15] introduced iterative exclusion methods, resulting in a 128 % increase in the number of identified lipids from the fourth iterative exclusion acquisition. However, satisfactory results were not achieved with all ion fragmentation acquisitions, which generated fragmentation ions without selecting the precursor ion.[40] These findings suggest the possibility of expanding lipid profile coverage, improving biomarker identification, and offering additional insights into diseases and treatment methods.[15]

Moreover, the study demonstrated that MS/MS fragmentation patterns can effectively identify ether-linked phospholipids. Plasmanyl-linked phospholipids exhibit a characteristic primary product ion, corresponding to the neutral loss of an *sn*2 acyl group as a ketene or a *sn*2 residue ion itself.[41–43] Notably, the neutral loss of the glycerol backbone in the *sn*2 acyl group leads to the neutral loss of H_3PO_4 from the sn1 plasmenyl group, resulting in the formation of a new C–N bond and rearrangement of the vinyl group.[41,44] The study further determined that the plasmenyl PE P-byproduct ions corresponded to the loss of the plasmenyl group ($RC{=}CH_2$) from the precursor ion and neutral loss of H_3PO_4 from the *sn*1 plasmenyl group. In this study, we employed TOF-MS for the semi-quantification of lipids, reflecting a relative change between each experimental group. While triple quadruple mass spectrometry is acknowledged as superior to TOF-MS in terms of quantification, Drotleff et al.[17] demonstrated that TOF-MS can provide quantifiable data. Specifically, we verified that the quantified data of PCs and SMs in the aorta can be utilized to assess the reproducibility of additional datasets.

Our study on the effects of EA treatment in SHR offers significant findings for hypertension treatment, but it has limitations. The focus on SHR may not directly apply to humans or other models, necessitating validation in diverse models or humans. While valuable, our reliance on in vivo methods and aortic lipid profiling using LC-MS provides limited insight into molecular mechanisms. Lack of a control group receiving sham treatment hinders attributing effects solely to EA. We predominantly focus on cardiovascular function, neural signaling, and aortic lipid profiles, potentially overlooking other pathways like immune system modulation or neuroendocrine pathways. Despite challenges, our investigation reveals noteworthy changes in lipid metabolites and key enzymes, offering insights into potential mechanisms associated with hypertension amelioration. Future research should employ more rigorous experimental designs, especially in molecular biology and neurology. This ongoing exploration aims to deepen understanding of how acupuncture may modulate hypertension and lipid metabolism.

These findings have implications for the clinical management of hypertension. The observed improvements in cardiovascular function and aortic lipid profiles in SHR with EA treatment suggest potential benefits for individuals with hypertension. Particularly, in acupuncture studies where metabolic and lipid profiles analyses are limited, this research provides insights into the mechanism of EA treatment for hypertension, guiding the possibility of personalized interventions through a comparison between EA treatment and conventional methods. The study highlights the potential for applying EA treatment directly to human subjects, suggesting that EA could be considered as an alternative or complementary approach to existing treatments.

The research findings are expected to potentially impact the clinical management of hypertension in patients. The results, indicating poten-

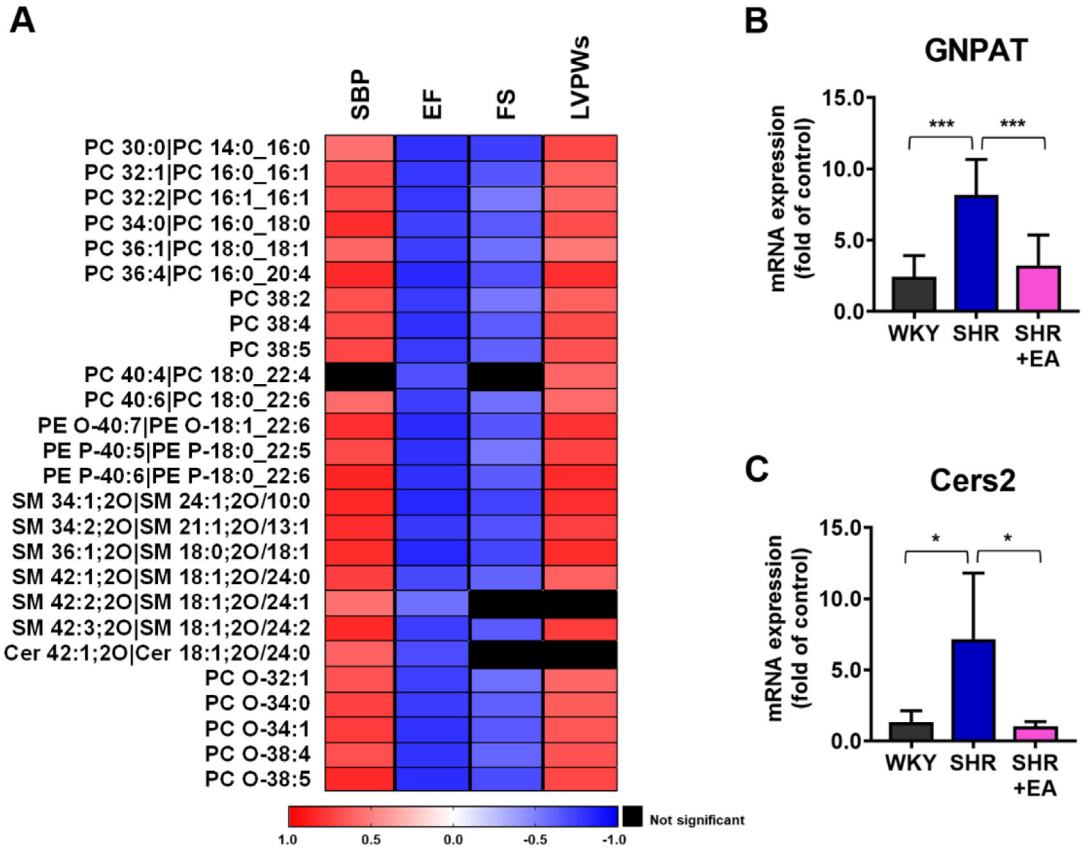

Fig. 8. Electroacupuncture treatment alters heart function-associated aortic lipids and mRNA expression of genes regulating lipid metabolism. (A) Correlation heat map between the selected aortic lipid metabolites and heart function indicators. Changes in (B) GNPAT and (C) Cers2 mRNA following six consecutive weeks of electroacupuncture treatment $^{*}p < 0.01$, $^{***}p < 0.001$. EA, electroacupuncture; WKY, Wistar-Kyoto rat; SHR, spontaneously hypertensive rat; SHR+EA, EA-treated SHR; SBP, Systolic blood pressure; LBPWs, left ventricular posterior wall thickness at end systole ejection fraction; PC, phosphatidylcholine; PC–O, plasmanyl-phosphatidylcholine; PE-O, plasmanyl- phosphoethanolamines; PE-P, plasmenyl-phosphoethanolamines; SM, sphingomyelin; Cer, ceramides; GNPAT, glyceronephosphate O-acyltransferase.

tial improvements in cardiovascular function and aortic lipid profiles in SHR with EA treatment, suggest possible benefits for individuals with hypertension. Particularly, in acupuncture studies where metabolic and lipid profile analyses are limited, this research provides insights into the mechanism of EA treatment for hypertension, guiding the possibility of personalized interventions through a comparison between EA treatment and conventional methods. The study highlights the potential for applying EA treatment directly to human subjects, suggesting that EA could be considered as an alternative or complementary approach to existing treatments.

This study introduces preliminary insights into the change in the aortic lipid profiles and cardiovascular parameters following EA treatment in SHR. The approach of LC-MS based lipid profile analysis as a tool provided a nuanced understanding of the lipid species alterations, including changes in plasmanyl PCs and ceramides. These findings suggest a potential pathway through which EA treatment may exert its effects, albeit with the acknowledgement that our results represent an initial exploration and should be interpreted with caution due to the limitations inherent in the experimental design and the small sample size. Given the exploratory nature of this research, further studies are warranted to build upon these initial observations. It is essential to conduct larger-scale investigations involving both animal models and human subjects to substantiate the impacts of EA on hypertension and its potential mechanisms. While this study contributes to the emerging discourse on the lipid profiles approach to understanding the effect of EA, we recognize the need for comprehensive research to validate and extend our findings. In light of the limitations highlighted and the preliminary state of our results, we advocate for cautious interpretation and consider this study as a stepping stone towards deeper investigations into the role of EA in hypertension management and its underlying mechanisms. This approach seeks to underline the importance of continued research in this area, aiming to contribute to the broader field of complementary and alternative medicine with robust, evidence-based findings in the future.

Author contributions

Hye-Yoom Kim: Data curation, Formal analysis, Investigation, Methodology, Writing-original draft. **Sarah Shin:** Data curation, Formal analysis, Investigation, Methodology, Writing-original draft. **Jung-Joo Yoon:** Formal analysis, Investigation, Methodology. **You-Mee Ahn:** Investigation, Formal analysis. **Ji-Hye Song:** Investigation, Formal analysis. **Da-Som Lee:** Investigation, Formal analysis **Ji-Yeun Park:** Investigation, Validation. **Ho-Sub Lee:** Supervison, Conceptualization, Project administration, Funding acquisition, Writing-review & editing. **Jeeyoun Jung:** Supervison, Conceptualization, Project administration, Validation, Funding acquisition, Writing-review & editing.

Declaration of competing interest

All authors declare that there are no conflicts of interest.

Funding

This research was supported by grants from the National Research Foundation of Korea (grant number: NFR-2017R1A5A2015805, NRF-2022R1A2C2092786), the Korea Institute of Oriental Medicine (grant number: KSN 2312021), and the Korea Health Technology R&D Project through the Korea Health Industry Development Institute (KHIDI) funded by the Ministry of Health and Welfare, Republic of Korea (grant number: RS-2020-KH088006).

Ethical statement

Not applicable.

Data availability

The data sets used and/or analyzed during the current study are available from the corresponding author on reasonable request.

Supplementary materials

Supplementary material associated with this article can be found, in the online version, at doi:10.1016/j.imr.2024.101041.

Fig S1. Linearity plot of internal standards (phosphatidylcholine, phosphatidyl-ethanolamine, and sphingomyelin).

Fig. S2. Semi-quantification results of significantly altered lipids by the EA treatment in SHR.

Table S1. Operational conditions and parameters of the UHPLC-Q-TOF MS system.

Table S2. PCR primer information.

Method S1. Immunostaining for hypertension-related neuronal signal analysis.

Method S2. Sample preparation for lipid profiling.

References

1. Sun Z. Aging, arterial stiffness, and hypertension. *Hypertension*. 2015;65(2):252–256. doi:10.1161/HYPERTENSIONAHA.114.03617.
2. Dugani SB, Moorthy MV, Li C, et al. Association of lipid, inflammatory, and metabolic biomarkers with age at onset for incident coronary heart disease in women. *JAMA Cardiol*. 2021;6(4):437–447. doi:10.1001/jamacardio.2020.7073.
3. Gebreyohannes EA, Bhagavathula AS, Abebe TB, Seid MA, Haile KT. In-hospital mortality among ischemic stroke patients in Gondar University Hospital: a retrospective cohort study. *Stroke Res Treat*. 2019;2019:7275063. doi:10.1155/2019/7275063.
4. Canoy D, Copland E, Nazarzadeh M, Ramakrishnan R, Pinho-Gomes AC, Salam A, et al. Antihypertensive drug effects on long-term blood pressure: an individual-level data meta-analysis of randomized clinical trials. *Heart*. 2022;108(16):1281–1289. doi:10.1136/heartjnl-2021-320171.
5. Stux G, Pomeranz B. *Acupuncture*. Berlin Heidelberg: Springer-Verlag; 2012.
6. W.H.O. Acupuncture: review and analysis of reports on controlled clinical trials. 2002.
7. Forouzanfar MH, Liu P, Roth GA, et al. Global burden of hypertension and systolic blood pressure of at least 110 to 115mmHg. *JAMA*. 2017;317(2):165–182. doi:10.1001/jama.2016.19043.
8. Li J, Sun M, Ye J, et al. The mechanism of acupuncture in treating essential hypertension: a narrative review. *Int J Hypertens*. 2019;2019:8676490. doi:10.1155/2019/8676490.
9. Kim DH, Ryu Y, Hahm DH, Sohn BY, Shim I, Kwon OS, et al. Acupuncture points can be identified as cutaneous neurogenic inflammatory spots. *Sci Rep.*. 2017;7(1):15214. doi:10.1038/s41598-017-14359-z.
10. Lopez JP, Nouri MZ, Ebrahim A, et al. Lipid profiles of urinary extracellular vesicles released during the inactive and active phases of aged male mice with spontaneous hypertension. *Int J Mol Sci*. 2022;23(23):15397. doi:10.3390/ijms232315397.
11. Chen S, Cheng W. Relationship between lipid profiles and hypertension: a cross-sectional study of 62,957 Chinese Adult Males. *Front Public Health*. 2022;10:895499. doi:10.3389/fpubh.2022.895499.
12. Dutta M, Joshi M, Srivastava S, Lodh I, Chakravarty B, et al. A metabonomics approach as a means for identification of potential biomarkers for early diagnosis of endometriosis. *Mol Biosyst*. 2012;8(12):3281–3287. doi:10.1039/c2mb25353d.
13. Au A, Cheng KK, Wei LK. Metabolomics, lipidomics and pharmacometabolomics of human hypertension. *Hypertension*. 2016;956:599–613. doi:10.1007/5584_2016_79.
14. Hinterwirth H, Stegemann C, Mayr M. Lipidomics: quest for molecular lipid biomarkers in cardiovascular disease. *Circ Cardiovasc Genet*. 2014;7(6):941–954. doi:10.1161/CIRCGENETICS.114.000550.
15. Koelmel JP, Kroeger NM, Gill EL, Ulmer CZ, Bowden JA, Patterson RE, et al. Expanding lipidome coverage using LC-MS/MS data-dependent acquisition with automated exclusion list generation. *J Am Soc Mass Spectrom*. 2017;28(5):908–917. doi:10.1007/s13361-017-1608-0.
16. Percie du Sert N, Hurst V, Ahluwalia A, et al. The ARRIVE guidelines 2.0: updated guidelines for reporting animal research. *PLoS Biol*. 2020;18(7):e3000410. doi:10.1371/journal.pbio.3000410.
17. Drotleff B, Illison J, Schlotterbeck J, Lukowski R, Lämmerhofer M. Comprehensive lipidomics of mouse plasma using class-specific surrogate calibrants and SWATH acquisition for large-scale lipid quantification in untargeted analysis. *Anal Chim Acta*. 2019;1086:90–102. doi:10.1016/j.aca.2019.08.030.
18. De Vet ECJM, Ijlst L, Oostheim W, Dekker C, Moser HW, van Den Bosch H, et al. Ether lipid biosynthesis: alkyl-dihydroxyacetonephosphate synthase protein deficiency leads to reduced dihydroxy acetonephosphate acyltransferase activities. *J Lipid Res*. 1999;40(11):1998–2003.
19. Schmidt S, Gallego SF, Zelnik ID, Kovalchuk S, Albæk N, Sprenger RR, et al. Silencing of ceramide synthase 2 in hepatocytes modulates plasma ceramide biomarkers predictive of cardiovascular death. *Mol Ther*. 2022;30(4):1661–1674. doi:10.1016/j.ymthe.2021.08.021.
20. Jin CN, Zhang TS, Ji LX, Tian YF. Survey of studies on mechanisms of acupuncture and moxibustion in decreasing blood pressure. *Zhongguo Zhen Jiu*. 2007;27(6):467–470.
21. Cui SY, Tang CZ. Progress in the research of neuroendocrine-immunological mechanism of acupuncture in regulating blood pressure and protecting target organs in hypertension. *Zhen Ci Yan Jiu*. 2008;33(3):208–212.
22. Wong WT, Wong SL, Tian XY, Huang Y. Endothelial dysfunction: the common consequence in diabetes and hypertension. *J Cardiovasc Pharmacol*. 2010;55(4):300–307. doi:10.1097/fjc.0b013e3181d7671c.
23. Hwang HS, Kim YS, Ryu YH, Lee JE, Lee YS, Yang EJ, et al. Electroacupuncture delays hypertension development through enhancing NO/NOS activity in spontaneously hypertensive rats. *Evid Based Complement Alternat Med*. 2011;2011:130529. doi:10.1093/ecam/nen064.
24. Lorell BH, Carabello BA. Left ventricular hypertrophy: pathogenesis, detection, and prognosis. *Circulation*. 2000;102(4):470–479. doi:10.1161/01.cir.102.4.470.
25. Palmiero P, Maiello M, Nanda NC. Is echo-determined left ventricular geometry associated with ventricular filling and midwall shortening in hypertensive ventricular hypertrophy? *Echocardiography*. 2008;25:20–26. doi:10.1111/j.1540-8175.2007.00564.x.
26. Romero CA, Orias M, Weir MR. Novel RAAS agonists and antagonists: clinical applications and controversies. Nature clinical practice. *Endocrinol Metabol*. 2015;11(4):242–252. doi:10.1038/nrendo.2015.6.
27. Tian GH, Sun K, Huang P, Zhou CM, Yao HJ, Huo ZJ, et al. Long-term stimulation with electroacupuncture at DU20 and ST36 rescues hippocampal neuron through attenuating cerebral blood flow in spontaneously hypertensive rats. *Evid Based Complement Alternat Med*. 2013;2013:482947. doi:10.1155/2013/482947.
28. Leung SB, Zhang H, Lau CW, Lin ZX. Attenuation of blood pressure in spontaneously hypertensive rats by acupuncture was associated with reduction oxidative stress and improvement from endothelial dysfunction. *Chin Med*. 2016;11:1–18. doi:10.1186/s13020-016-0110-0.
29. Jung J, Lee SM, Lee MJ, Ryu JS, Song JH, Lee JE, et al. Lipidomics reveals that acupuncture modulates the lipid metabolism and inflammatory interaction in a mouse model of depression. *Brain Behav Immun*. 2021;94:424–436. doi:10.1016/j.bbi.2021.02.003.
30. Liu CC, Chen JL, Chang XR, He QD, Shen JC, Lian LY, et al. Comparative metabolomics study on therapeutic mechanism of electro-acupuncture and moxibustion on rats with chronic atrophic gastritis (CAG). *Sci Rep*. 2017;7(1):1–11. doi:10.1038/s41598-017-13195-5.
31. Mulders AC, Hendriks-Balk MC, Mathy MJ, Michel MC, Alewijnse AE, Peters SL. Sphingosine kinase–dependent activation of endothelial nitric oxide synthase by angiotensin II. *Arterioscler Thromb Vasc Biol*. 2006;26(9):2043–2048. doi:10.1161/01.ATV.0000237569.95046.b9.
32. Mulders A, Mathy MJ, Meyer zu Heringdorf D, ter Braak M, Hajji N, Olthof DC, et al. Activation of sphingosine kinase by muscarinic receptors enhances NO-mediated and attenuates EDHF-mediated vasorelaxation. *Basic Res Cardiol*. 2009;104(1):50–59. doi:10.1007/s00395-008-0744-x.
33. Borodzicz S, Czarzasta K, Kuch M, Cudnoch-Jedrzejewska A. Sphingolipids in cardiovascular diseases and metabolic disorders. *Lipids Health Dis*. 2015;14:55. doi:10.1186/s12944-015-0053-y.
34. Spijkers LJ, van den Akker RF, Janssen BJ, Debets JJ, De Mey JG, Stroes ES, et al. Hypertension is associated with marked alterations in sphingolipid biology: a potential role for ceramide. *PLoS ONE*. 2011;6(7):e21817. doi:10.1371/journal.pone.0021817.
35. Maceyka M, Spiegel S. Sphingolipid metabolites in inflammatory disease. *Nature*. 2014;510(7503):58–67. doi:10.1038/nature13475.
36. Drin G. Topological regulation of lipid balance in cells. *Annu Rev Biochem*. 2014;83:51–77. doi:10.1146/annurev-biochem-060713-035307.
37. Dietrich S, Floegel A, Weikert C, Prehn C, Adamski J, Pischon T, et al. Identification of serum metabolites associated with incident hypertension in the European Prospective Investigation into Cancer and Nutrition-Potsdam Study. *Hypertension*. 2016;68(2):471–477. doi:10.1161/HYPERTENSIONAHA.116.07292.
38. Dorninger F, Forss-Petter S, Berger J. From peroxisomal disorders to common neurodegenerative diseases—the role of ether phospholipids in the nervous system. *FEBS Lett*. 2017;591(18):2761–2788. doi:10.1002/1873-3468.12788.
39. Braverman NE, Moser AB. Functions of plasmalogen lipids in health and disease. *Biochim Biophys Acta Mol Basis Dis*. 2012;1822(9):1442–1452. doi:10.1016/j.bbadis.2012.05.008.
40. Naz S, Gallart-Ayala H, Reinke SN, Mathon C, Blankley R, Chaleckis R, et al. Development of a liquid chromatography-high resolution mass spectrometry metabolomics method with high specificity for metabolite identification using all ion fragmentation acquisition. *Anal Chem*. 2017;89(15):7933–7942. doi:10.1021/acs.analchem.7b00925.

41. Khaselev N, Murphy RC. Electrospray ionization mass spectrometry of lysoglycerophosphocholine lipid subclasses. *J Am Soc Mass Spectrom*. 2000;11(4):283–291. doi:10.1016/S1044-0305(99)00158-0.
42. Hsu FF, Turk J. Differentiation of 1-O-alk-1′-enyl-2-acyl and 1-O-alkyl-2-acyl glycerophospholipids by multiple-stage linear ion-trap mass spectrometry with electrospray ionization. *J Am Soc Mass Spectrom*. 2007;18(11):2065–2073. doi:10.1016/j.jasms.
43. Koch J, Lackner K, Wohlfarter Y, Sailer S, Zschocke J, Werner ER, et al. Unequivocal mapping of molecular ether lipid species by LC-MS/MS in plasmalogen-deficient mice. *Anal Chem*. 2020;92(16):11268–11276. doi:10.1021/acs.analchem.0c01933.
44. Berry KAZ, Murphy RC. Electrospray ionization tandem mass spectrometry of glycerophosphoethanolamine plasmalogen phospholipids. *J Am Soc Mass Spectrom*. 2004;15(10):1499–1508. doi:10.1016/j.jasms.2004.07.009.